Journal of Hydrology 582 (2020) 124452

Contents lists available at ScienceDirect

Journal of Hydrology

journal homepage: www.elsevier.com/locate/jhydrol

Research papers

Runoff and sediment production from harvested hillslopes and the riparian area during high intensity rainfall events

Kira C. Puntenney-Desmond[a], Kevin D. Bladon[a,*], Uldis Silins[b]

[a] Department of Forest Engineering, Resources, and Management, Oregon State University, Corvallis, OR, USA
[b] Department of Renewable Resources, University of Alberta, Edmonton, AB, Canada

ARTICLE INFO

This manuscript was handled by Marco Borga, Editor-in-Chief, with the assistance of Felix Frances, Associate Editor

Keywords:
Erosion
Forest harvesting
Hillslope hydrology
Rainfall simulation
Runoff
Rocky Mountains

ABSTRACT

Forest harvesting often decreases soil infiltration capacity, leading to rapid and increased delivery of surface runoff, shallow subsurface runoff, and sediment to streams. While the general harvest area is typically the largest area of disturbance, relative to forest roads or skid trails, less is known about the degree to which the general harvest areas act as sources or sinks for runoff and sediment transport. This includes a need to improve understanding of the potential for runoff and sediment delivery from harvest areas through riparian buffers to streams during infrequent, high intensity precipitation events, which are predicted to increase due to climate change. In this study, we used rainfall simulations to investigate surface/shallow subsurface runoff, and sediment transport from plots during extreme precipitation events within a steep, headwater catchment in the Rocky Mountains. Simulations consisted of one hour of high intensity rainfall (I_{60}: 70–80 mm h^{-1}), representative of an ~100 year, or greater, storm event for the northern Rocky Mountain region. Our objectives were to compare runoff rates, sediment concentrations, and sediment yields between the general harvest area, along the edge of the riparian buffer at the interface with the harvested area, and within the riparian buffer. Surface/shallow subsurface runoff rates were greatest in the riparian buffer relative to the harvest area, especially when soil conditions were dry. Mechanical soil disturbance during forest harvesting appeared to result in higher infiltration rates and vertical, preferential flow relative to the riparian buffer. However, sediment concentrations in runoff from plots in the general harvest area were ~15.8-times greater than in the riparian buffer and ~4.2-times greater than at the harvest-riparian edge. Comparatively, sediment yields in the general harvest area were ~2.0-times greater than in the riparian buffer and ~1.2-times greater than at the harvest-riparian edge. Quantitative and qualitative evidence suggests differences in runoff and sediment between the harvest area, harvest-riparian edge, and riparian buffer were due to site differences in hydrophobicity, surface roughness, soil water content, and sediment supply. While we observed moderately high variability with only modest replication, the spatial patterns in the amount and timing of runoff, sediment production, and their relationships with soil moisture were consistent and monotonic along the gradient from harvested areas through riparian buffers. This highlights the need for additional research to explore if similar patterns appear evident after forest harvesting in other hydro-climatic settings.

1. Introduction

Forest disturbances due to human activities (e.g., resource extraction) or natural processes (e.g., wildfire, pest outbreaks) can have spatially extensive and long lasting effects on hydrologic and ecosystem processes (Ebel and Mirus, 2014; Mirus et al., 2017). The hydrological consequences of forest disturbance include changes in rates of interception, evapotranspiration, soil moisture dynamics, groundwater recharge, and annual discharge, baseflows, and peak flows (Bladon et al., 2019; Hallema et al., 2017; Jones et al., 2012; Moore and Wondzell, 2005). Reductions in forest canopy cover can also lead to increased net precipitation and changes in soil hydraulic properties, often resulting in elevated erosion and sediment delivery to streams (Goode et al., 2012; Silins et al., 2009). Such shifts in the delivery and transport of both water and sediment from disturbed hillslopes into mountain streams can degrade water quality for both aquatic habitat and downstream water resource management (Emelko et al., 2011; Emelko et al., 2016).

The hydrologic effects of forest harvesting activities, in particular, have been the focus of scientific investigation for decades (Bosch and Hewlett, 1982; Brown et al., 2005; Stednick, 1996). The majority of

* Corresponding author at: 280 Peavy Hall, College of Forestry, Oregon State University, Corvallis, OR 97331, USA.
E-mail address: bladonk@oregonstate.edu (K.D. Bladon).

https://doi.org/10.1016/j.jhydrol.2019.124452
Received 1 July 2019; Received in revised form 10 October 2019; Accepted 9 December 2019
Available online 16 December 2019

research has focused on the most compacted surfaces—roads and skid trails (Luce, 2002; Sheridan et al., 2006; Sosa-Perez and MacDonald, 2017). These highly compacted surfaces decrease the soil infiltration capacity, leading to more rapid and increased delivery of surface runoff, shallow subsurface runoff, and sediment to the stream (Luce and Black, 1999; MacDonald et al., 2001). Research has shown an increase of ~2- to 100-times more runoff and sediment from roads and skid trails compared to undisturbed surfaces, even during low intensity rain events (Croke et al., 1999a; Luce and Black, 1999). Moreover, many studies have found that unpaved haul roads or skid trails in steep, unstable terrain can increase the occurrence of mass movements by 25- to 350-times (Amaranthus et al., 1985; Gray and Megahan, 1981; Wemple et al., 2001), increasing the delivery of sediment to stream channels (Benda et al., 2005; Brardinoni et al., 2003).

However, the general harvest area (i.e., area of tree harvesting, excluding primary skid trails and haul roads) typically represents a much greater area of disturbance relative to forest roads or skid trails and harvesting activities also impact this area, especially if ground-based forest-harvesting equipment is used (Ampoorter et al., 2012; Miller et al., 1996). Heavy machinery, such as harvesters, skidders, and forwarders, can compact soils, increase bulk density, and decrease air-filled porosity, infiltration capacity, and hydraulic conductivity across the general harvest area (Mohr et al., 2013; Sidle et al., 2006). These effects are spatially heterogeneous, leading to uncertainties about the contribution of the harvest area to runoff and sediment (Croke et al., 1999a; Croke et al., 1999b). For example, in the first two years after forest harvesting Oyarzun and Pena (1995) observed 1.8- to 3.9-times greater runoff and 1.9- to 5.8-times greater sediment concentrations from harvested plots compared to undisturbed *Pinus radiata* (Monterey pine) forest plots. In contrast, Hartanto et al. (2003) observed ~48% less runoff and ~54% less soil loss from harvested plots compared to undisturbed plots in Indonesian rainforest catchments. Thus, the degree to which the general harvest areas act as sources or sinks for runoff and sediment transport remains unclear (Mohr et al., 2013; Wallbrink and Croke, 2002).

Historical research (1950s and 1960s) on the effects of forest management illustrated that the general harvest area could act as a principal source of increased runoff and sediment (Brown and Krygier, 1971; Fredriksen, 1970; Harris, 1977). The results from these early studies led to legislation requiring retention of riparian vegetation around streams to protect the freshwater environment (Cristan et al., 2016). Recent studies suggest that current best management practices (BMPs), including retention of a riparian buffer, are mostly effective at reducing the potential for sediment from general harvest areas to reach streams and negatively impact water quality and aquatic habitat (Hatten et al., 2018; Litschert and MacDonald, 2009). However, there are still instances where harvest units following contemporary forest harvesting practices can provide a source of sediment (Bywater-Reyes et al., 2017; Macdonald et al., 2003; Motha et al., 2003), indicating a need to better understand processes and drivers of runoff and sediment production from general harvest areas into or through riparian buffers.

Furthermore, projections suggest climate change may lead to increased precipitation amounts and intensities in many regions (Easterling et al., 2000; Trenberth et al., 2003). This may result in higher rainfall erosivity, amplified runoff response, and increased erosion rates (Praskievicz, 2016; Routschek et al., 2014). Model simulations by Ramos and Martinez-Casasnovas (2015), based on mid-range climate change scenarios (HadCM3 A2) in a Mediterranean climate, indicate an increase in soil loss as high as 12% by 2020 and 57% for 2050. Similarly, models by Nearing et al. (2004) project an increase in erosion of ~1.7% for each 1% change in annual precipitation, in part due to wetter soil conditions and higher water tables. Improved understanding of the processes linking runoff and sediment delivery to streams during infrequent, high intensity precipitation events are needed to help frame the scope of these predictions in forested environments.

Here, we provide insights into the role of the general harvest area and riparian buffer as sources or sinks for runoff and sediment transport during high intensity precipitation events. Specifically, in this study, we investigated surface/shallow subsurface runoff, and sediment transport from plots during extreme precipitation events within a steep, headwater catchment, recently harvested in the Rocky Mountains. Our objectives were to evaluate and compare runoff rates, sediment concentrations, and sediment yields during high intensity precipitation events between the general harvest area, along the edge of the riparian buffer at the interface with the harvested area, and within the riparian buffer. Specifically, we used rainfall simulations of high intensity, short duration storm events to (a) quantify surface or shallow sub-surface runoff rates, (b) quantify sediment concentrations and yields, and (c) determine the influence of antecedent soil moisture on both runoff and sediment production within the general harvest area, along the riparian buffer edge, and within the riparian buffer.

2. Methods

2.1. Study area

Star Creek is a 10.3 km^2 headwater catchment on the eastern slopes of the Rocky Mountains of southwest Alberta, Canada (49° 37′ N, 114° 40′ W) (Fig. 1). The catchment is predominantly northeast-facing with basin elevation ranging from 1479 to 2627 m. The average catchment slope is ~45%, while the average channel slope is ~11% (Wagner et al., 2014). Forest vegetation in the study catchment is dominated by stands of lodgepole pine (*Pinus contorta* var. *latifolia*), trembling aspen (*Populus tremuloides*), and Douglas-fir (*Pseudotsuga menziesii* var. *glauca*) at lower elevations (upper montane). At mid-elevations (sub-alpine), the vegetation is characterized by Engelmann spruce (*Picea engelmanii*) and subalpine fir (*Abies lasiocarpa*), while high elevations are alpine meadow vegetation transitioning to talus slopes and bare rock. Soils are well to imperfectly drained Eutric or Dystric Brunisols (Inceptisols [U.S. Soil Taxonomy]), with weak soil horizon development typical of higher elevation northern environments. Geology is primarily Cretaceous shale, sandstone, mudstone, and limestone.

Winters are typically cold (mean monthly air temperature: −7 °C) and summers are mild (mean monthly air temperature: 16 °C). The mean annual air temperature is ~4.6 °C. The mean annual precipitation ranges between 800 and 1360 mm $year^{-1}$, with mean annual streamflow ranging from 600 to 1225 mm $year^{-1}$ (Silins et al., 2016). Precipitation predominantly falls as snow between October and April (50–70%), leading to peak streamflow as snowmelt in May–June (Mahat and Anderson, 2013).

Star Creek West, a 458 ha sub-basin of the Star Creek catchment, was harvested as a variable retention clearcut between January–March 2015. Forest harvesting operations consisted of the removal of 62 ha of timber using ground-based equipment where felled trees were skidded to landings for processing. Following harvesting, the cutover areas were drag scarified (dozer /anchor chain) and left for natural regeneration. This harvest treatment represented contemporary forest management practices in the region and was being compared with two alternative harvesting treatments in the other two sub-basins of the Star Creek catchment as part of the Southern Rockies Watershed Project study (Silins et al., 2016). Operable areas were restricted to slopes less than 45%. A 30 m riparian buffer was retained around all mapped waterbodies.

2.2. Rainfall simulation plots

We selected 15 plots for rainfall simulations along three transects on a north facing hillslope (aspect: ~358°) and along two transects on a southeast facing hillslope (aspect: ~129°) (Fig. 1). Each transect consisted of three plots that were spaced ~20 m apart along the planar hillslopes. Each plot was one square-meter, which was bounded by a

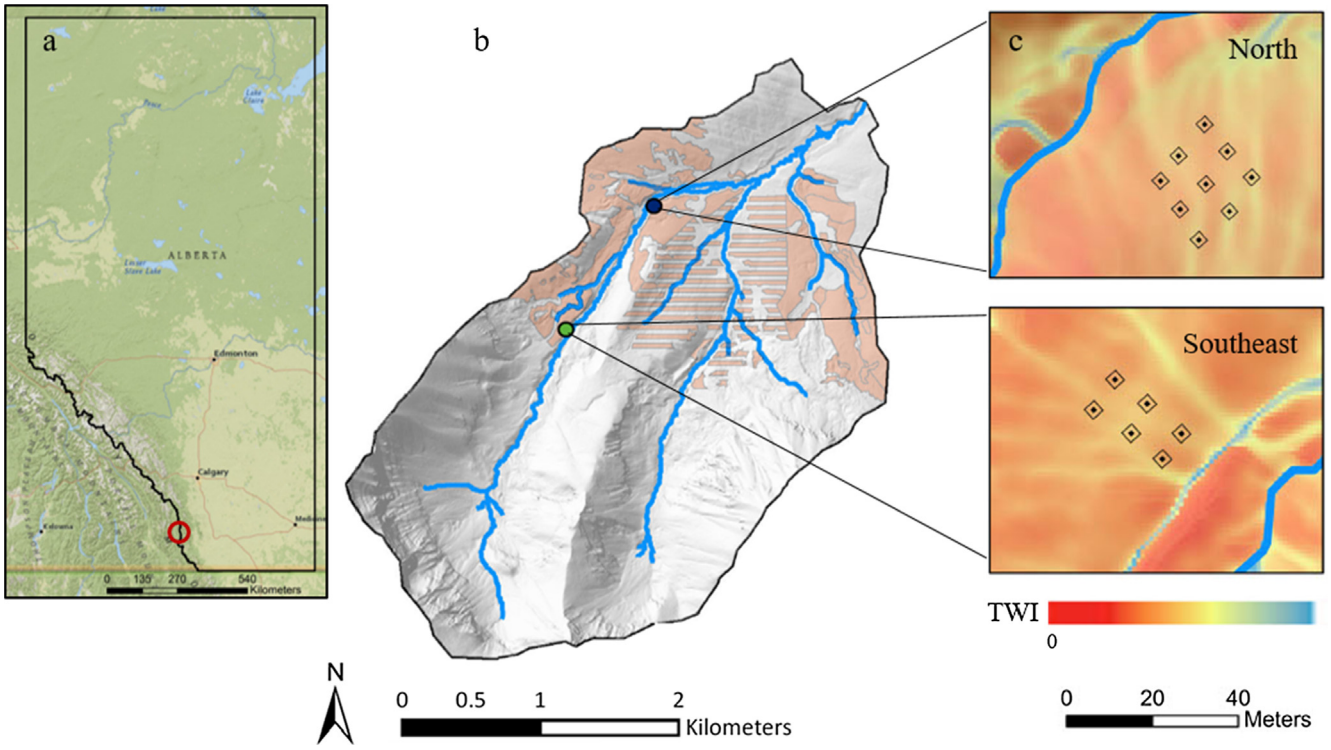

Fig. 1. Map of (a) the province of Alberta with the general location of Star Creek (red circle), (b) the Star Creek catchment, indicating the locations for the rainfall simulation sites and the area of the catchment (orange), and (c) the locations of rainfall simulation plots at the north site and southeast site with topographic wetness indices (TWI). (For interpretation of the references to colour in this figure legend, the reader is referred to the web version of this article.)

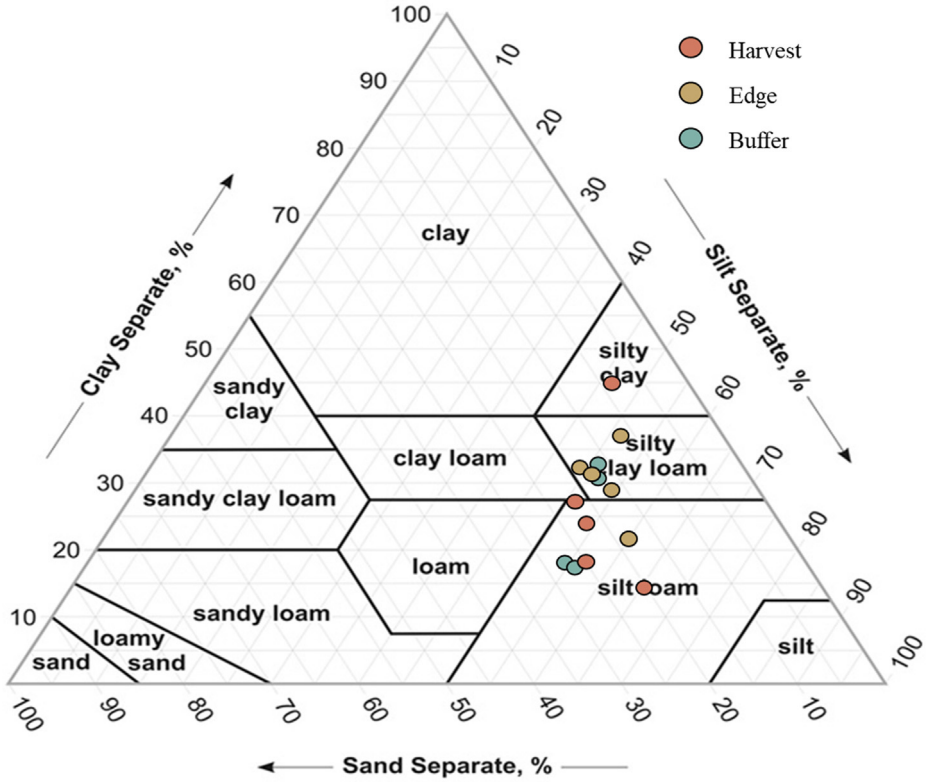

Fig. 2. Soil texture of the fine fraction for each of the 15 simulation plots.

Table 1
Summary of plot characteristics (mean and standard error) for the north-facing site, southeast-facing site, and all sites combined within the general harvest area, along the harvest-riparian edge, and in the riparian buffer.

Plot Position	Plot #	Slope (%)	Dry VMC		Wet VMC		Canopy Closure (%)	Foliar Cover (%)	Litter Depth (cm)	BareSoil (%)
			θ_{or} (%)	θ_m (%)	θ_{or} (%)	θ_m (%)				
Harvest Area	1	13	7.9	26.7	13.8	36.1	12	–	6	–
	2	25	18.4	25.1	31.4	28.5	17	12	5	6
	3	28	23.7	24.6	30.1	35.0	26	48	6	0
	4	29	17.4	17.2	31.9	32.7	13	38	4	0
	5	26	12.1	23.1	28.6	33.6	7	16	5	2
Harvest-Riparian Edge	6	42	18.0	17.0	–	–	41	28	5	0
	7	34	4.8	13.1	20.3	15.0	64	12	4	0
	8	35	19.4	23.3	39.9	36.8	52	30	3	0
	9	39	23.1	16.9	38.6	21.6	50	48	5	0
	10	26	5.9	13.2	13.1	22.9	38	14	8	0
Riparian Buffer	11	46	4.1	8.3	21.7	17.7	80	24	3	0
	12	36	9.4	8.1	9.8	14.7	89	40	2	0
	13	37	7.8	8.6	25.3	18.3	85	52	6	0
	14	50	6.2	7.3	23.6	19.7	90	54	9	0
	15	55	11.7	8.0	16.2	13.9	84	32	9	0

three-sided steel frame that was inserted into the soil with the open side facing down the slope. The plots were located either (a) within the general harvest area, (b) along the edge of the riparian buffer at the interface with the harvested area, or (c) within the riparian buffer.

We characterized each of the 15 plots based on soil texture (Fig. 2), aspect, local slope, canopy closure, foliar and ground cover, and litter depth (Table 1). The soil particle distribution for the sand, silt, and clay fraction was determined in the laboratory using the hydrometer method (Gee and Or, 2002). Soil texture for the fine fraction (< 2 mm) of the upper 0–6 cm of mineral soil was similar along the north-facing and southeast-facing hillslopes, ranging from silty loam to silty clay loam (Fig. 2). Soil samples contained poorly sorted rocks and gravel, estimated to make up ~2–20% of the sample volume.

Local plot slopes generally increased from the general harvest area into the riparian buffer (Table 1). Slopes ranged from 13 to 29% within the harvested area, 26–42% at the riparian-harvest boundary, and 36–55% within the riparian buffer. Canopy closure, which is a measure of the portion of the sky hemisphere obscured by the vegetative canopy, was estimated using a spherical concave densiometer held at the center of each plot. Canopy closure also increased from the general harvest area (~15%), to the buffer-harvest edge (~49%), and into the riparian buffer (~86%). Foliar and ground cover was estimated within each plot from 50 points along a 10 cm^2 sampling grid using the line point intercept method (Bonham, 2013). Foliar cover classes included grasses, forbs, and shrubs. Ground cover classes included litter/slash, moss, wood, rocks, and bare ground. Foliar cover was generally greater on the south-east facing slope compared to the north facing slope—it was ~3.1-times greater in the general harvest area, 2.2-times greater along the buffer-harvest edge, and 1.7-times greater in the riparian buffer (Table 1). We quantified litter depth (O-horizon) by measuring the depth from the forest floor surface to the surface of the mineral soil (A horizon) at three points along the exposed soil face at the bottom edge of each plot. We then averaged the three point measurements for each plot. Litter depths ranged from 2 to 9 cm, but were similar between the general harvest area, buffer-harvest edge, and in the riparian buffer. Mean upslope accumulated area above each of the 1 m^2 plots was 63.3 ± 14.0 m^2 for the harvested plots, 44.4 ± 6.0 m^2 for the buffer-harvest edge plots, 54.4 ± 6.3 m^2 for the buffer plots.

2.3. Rainfall simulations

We conducted two rainfall simulations on each of the 15 plots—once under dry antecedent moisture conditions and once under wet antecedent moisture conditions during August 2015. Simulations consisted of one hour of high intensity rainfall (I_{60}: 70–80 mm h^{-1}), representative of a 100 year return period, or longer, storm event for the northern Rocky Mountain region. The return period for the storm event was estimated using rainfall frequency analysis (Weibull formula) with an annual maximum precipitation series from a centrally located precipitation gauge. Following the first (dry conditions) simulation, the plot remained uncovered for 24-hr prior to performing the second (wet conditions) simulation.

The rainfall simulator design was adopted and modified from Covert and Jordan (2009) as a robust, portable device well suited for remote, steep terrain (Fig. 3). The simulator consisted of a single wide-angle spray nozzle (1/2HH-30WSQ, Spraying Systems Co., Wheaton, Illinois) mounted to the bottom of a small platform. The platform was mounted on a tripod base that extended to 3 m height above the plot, which was found to produce rainfall velocities that were representative of high intensity, short duration, convective storms that are common in the study region (Covert and Jordan, 2009). The water supply for simulations was drawn directly from the adjacent stream using a water pump (Honda WX 15, American Honda Power Equipment Division, Alpharetta, GA) positioned at the base of the riparian buffer to deliver water to the nozzle through 30 m of 3.8 cm diameter flat hose and 15 m of 1.6 cm diameter garden hose. This design provided a continuous water supply to maintain the target rainfall intensity over the one-hour simulation. The pump intake was screened to minimize the potential for coarse debris to clog the system. Given that simulations occurred during baseflow conditions in August, we assumed negligible fine sediment contribution from the stream water. However, we collected a composite water sample during simulations from two rain gauges (Model 6331 Manual Stratus Rain Gauge) placed on opposite corners of the plot, to confirm that fine sediment in the simulated precipitation was insignificant.

2.4. Runoff and sediment samples

During each rainfall simulation, we collected five surface/shallow subsurface runoff samples from the bottom edge of the plot. These runoff samples were a combination of near-surface biomat flow (Sidle et al., 2007), surface runoff, and shallow subsurface flow (upper ~5 cm of soil). Water samples were collected in 500 ml polyurethane bottles from a trough, which was connected to the hillslope with a 0.04 cm metal sheet inserted at the boundary between the organic layer and mineral soil horizon. While a small amount of disturbance occurred directly at the interface with the metal insert, installation was standardized across all plots to prevent introduction of bias into runoff

Fig. 3. Photographs of the (a) rainfall simulator extended above the 1 m^2 plot, (b) rainfall simulator nozzle and pressure gauge, and (c) runoff into the trough at the base of the plot showing the metal apron slotted into the organic-mineral soil horizon.

results. Samples were collected at 12-minute intervals. The amount of time required to fill each bottle varied. Thus, a single bottle was used to capture runoff during each collection interval, either until the bottle filled or the 12 min had elapsed. We recorded the time of runoff initiation as time from the start of the simulation to the moment when runoff first exited the collection trough. The collection trough was shielded from above during rainfall simulation with a clear Plexiglas cover, while the plots were bounded on three sides with a steel frame to ensure only runoff from within the plot contributed to the water sample.

Sample volumes and total sediment concentrations were determined in the laboratory following field collection. Runoff samples were first passed through a 250 μm sieve to remove large particulates and then filtered using a vacuum pump and 0.7 μm glass microfiber filters (Whatman grade GF/F). Prior to weighing the filters to determine the total mass of sediment, we removed the organic fraction through loss on ignition by placing the filters in a muffle furnace at 450 °C for three hours. Sediment concentrations were calculated as the mass (mg) of sediment per unit volume (L) of runoff collected. Sediment yields (mg m^{-2} min^{-1}) were calculated as the product of sediment concentration (mg L^{-1}) and plot discharge (L min^{-1}) divided by the plot area (1 m^2).

2.5. Soil water content

The baseline soil content conditions of the organic (O) and mineral soil horizons were determined directly preceding (pre-) and following (post-) each simulation to characterize antecedent and post-rainfall soil moisture. The volumetric water content of the O-horizon (θ_{or}) was measured at two points adjacent to the exterior edge of the plot frame. The O-horizon sample was collected by removing a 5 cm^2 area of the O-horizon down to the mineral soil and averaging the depth at four points to obtain a known volume for each sample. We re-filled the void created when extracting the O-horizon bulk density sample with representative organic matter to keep the forest floor cover as continuous as possible during the simulation. Water content of each sample was then determined in the laboratory by weighing the sample before and after oven-drying at 40 °C for 3–5 days.

The volumetric water content of the upper 0–6 cm of the mineral soil horizon (θ_m) was measured vertically at six points evenly distributed around the exterior edge of the plot frame with an impedance soil moisture probe (ML3 ThetaProbe, Delta T-Devices, Cambridge, UK, accuracy: ± 1%). The mineral soil surface was exposed for each reading by carefully displacing the O-horizon. For each reading, we averaged three point measurements to account for high spatial variability in θ_m. The O-horizon was then replaced to cover the mineral soil during rainfall simulation. As both the organic and mineral sampling procedures caused disturbance to the soil, measurements were taken from unique (slightly offset) locations at each of the four sampling periods (i.e., pre-dry, post-dry, pre-wet, post-wet).

2.6. Statistical analysis

We used one-way analysis of variance (ANOVA) to test for differences in means of runoff rates, sediment concentrations, sediment yields, and soil water content. Assumptions of equal variance, normality, and independence in each of the data sets were evaluated; sediment concentrations and yields exhibited skewed distributions and were log-transformed for statistical tests.

While aspect was initially explored as a potential factor, response variables were unrelated to aspect and all five transects were pooled to explore the effect of plot position (i.e., general harvest area, harvest-riparian edge, riparian buffer). Pseudoreplication in the study design was addressed by conducting independent tests for each of the time periods or soil moisture conditions (i.e., pre-, post-, dry, wet). The five runoff samples collected during each simulation were repeated measures, producing temporal autocorrelation in the repeated sampling data. As a result, statistical comparisons among sites used the aggregate

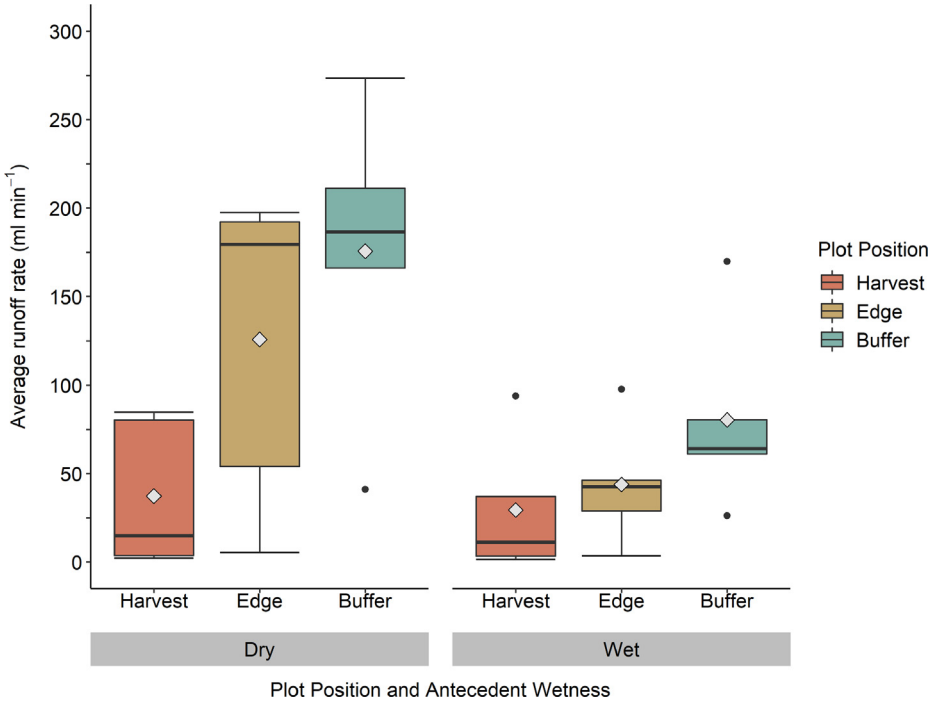

Fig. 4. Box-and-whisker plots of the average runoff rate from plots in the general harvest area, at the harvest-riparian edge, and in the riparian buffer plots during the dry and wet rainfall simulations. Grey dots indicate the arithmetic means.

mean runoff rate and geometric mean sediment concentration or yield (back transformation of log values) from each simulation. Post-hoc comparisons between means of the general harvest area, buffer-harvest edge, and riparian buffer were conducted using Tukey HSD tests. Statistical significance was assessed at a threshold of $\alpha = 0.05$. All statistical analyses were performed in R version 3.4.0 (R Core Team, 2017).

3. Results

3.1. Runoff rates

During the dry condition rainfall simulations the general pattern of runoff rates (surface/shallow subsurface flow) was riparian buffer (175.6 ± 17.3 [SE] ml min^{-1}) > harvest-riparian edge (125.8 ± 18.2 ml min^{-1}) > general harvest area (37.2 ± 8.5 ml min^{-1}) (Fig. 4). Mean runoff rates within the riparian buffer plots were greater than within the general harvest area plots ($t = 2.90, p = .03$). Runoff rates along the riparian edge appeared to be transitional between the harvest area and the riparian buffer with no difference in the runoff rates between the harvest-riparian edge and the general harvest area ($t = 1.86$, $p = .19$) or the riparian buffer ($t = 1.05, p = .56$).

The surface/shallow subsurface runoff rates decreased in all plots during the wet condition rainfall simulations relative to the dry simulation runoff rates. While the general pattern of mean runoff rates remained the same (Fig. 4)—riparian buffer (83.6 ± 9.9 [SE] ml min^{-1}) > harvest-riparian edge (40.4 ± 6.8 ml min^{-1}) > general harvest area (29.4 ± 10.2 ml min^{-1}), variation in wet runoff rates among plot positions was comparatively weak ($p > .25$ for all pairwise comparisons).

Not surprisingly, runoff ratios, calculated as the fraction of total precipitation collected as surface/shallow subsurface runoff, followed a similar pattern as the basic runoff rates (Table S2). Runoff ratios were only statistically greater in the riparian buffer plots (13.9 ± 3.1%) relative to the general harvest area (2.9 ± 1.5%) during the dry condition rainfall simulations ($t = 2.9; p = .03$). Comparisons in runoff ratios between all other plot positions were weaker ($p > .20$). Similarly, all runoff ratios declined during the wet condition rainfall simulations relative to the dry condition simulations with no evidence for differences between any of the plot positions ($p > .27$ for all pairwise comparisons).

In contrast, while the variation among plot positions was weaker, the general pattern of time to surface/shallow subsurface runoff initiation after the start of rainfall simulations under dry and wet conditions was opposite of that observed for runoff rate. Time of runoff initiation under the dry condition rainfall simulations was approximately the same in the riparian buffer plots (2.02 ± 0.39 [SE] mins) and the harvest-riparian edge plots (1.89 ± 0.26 mins), and only marginally longer in the harvest area plots (3.66 ± 1.08 mins) (Fig. 5; all pairwise comparisons $p > .18$). However, during the wet condition rainfall simulations, it took longer for surface/shallow subsurface runoff to initiate and a weak pattern of time to runoff initiation was apparent. The time to runoff initiation was shortest in the riparian buffer (2.38 ± 0.45 [SE] mins) followed by the plots at the harvest-riparian edge (3.76 ± 0.46 mins) and the general harvest area (5.12 ± 1.14 mins) (Fig. 5; Fig. S2). Again, none of these comparisons were significant at $\alpha = 0.05$ ($p > .10$).

3.2. Sediment concentrations and yields

During the dry condition rainfall simulations the general patterns of sediment concentrations and sediment yields were opposite of the runoff rates, with the general harvest area > harvest-riparian edge > riparian buffer (Fig. 6). Specifically, the geometric mean and 95% confidence intervals (back-transformed) for the sediment concentration was (a) 424.8 mg l^{-1} (151.0–1195.3 mg l^{-1}) in the general harvest area, (b) 100.9 mg l^{-1} (45.8–222.1 mg l^{-1}) along the harvest-riparian edge, and (c) 26.9 mg l^{-1} (12.2–59.1 mg l^{-1}) in the riparian buffer. Statistically, there was strong evidence for differences in sediment concentrations between the general harvest area and along the harvest-riparian edge ($t = 3.21, p = .01$) and between the harvest area and the riparian buffer ($t = 6.17, p < .001$). There was moderate

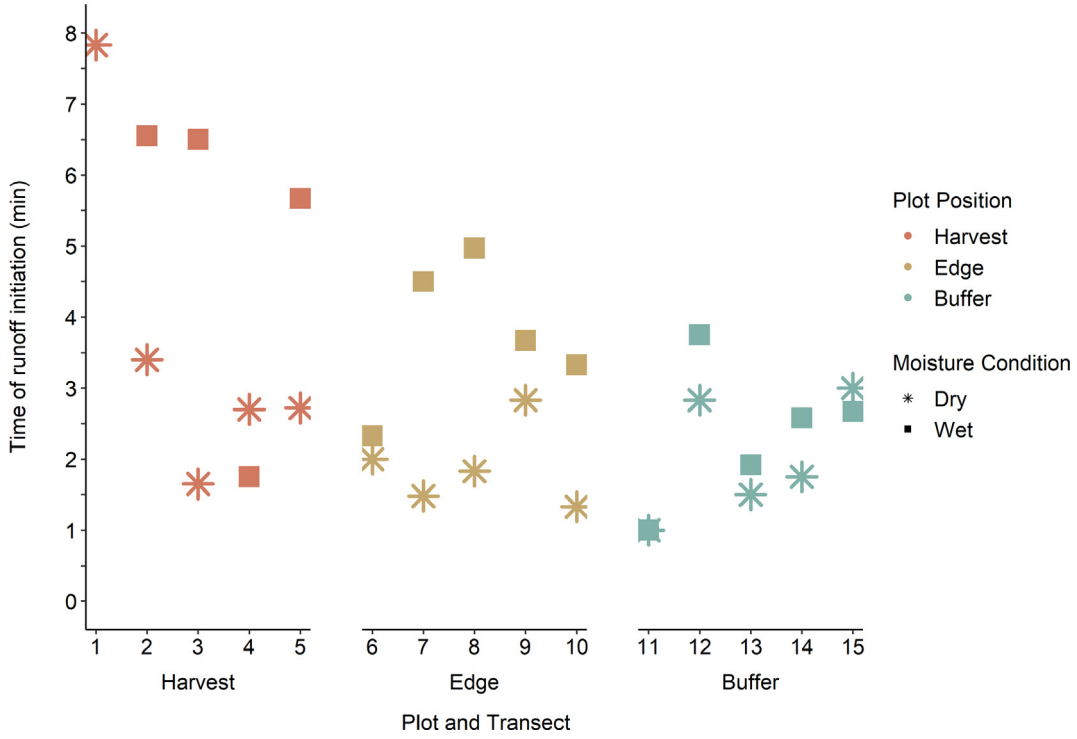

Fig. 5. Time of runoff initiation from the start of the rainfall simulation under dry and wet antecedent soil moisture conditions from plots in the general harvest area (plots 1–5), at the harvest-riparian edge (plots 6–10), and in the riparian buffer (plots 11–15).

evidence for differences between the harvest-riparian edge and the riparian buffer (t = 2.96, p = .03). The geometric mean and 95% confidence intervals (back-transformed) for the sediment yields during the dry simulations was (a) 7.3 mg m^{-2} min^{-1} (0.7–46.2 mg m^{-2} min^{-1}) in the general harvest area, (b) 5.9 mg m^{-2} min^{-1} (1.6–34.3 mg m^{-2} min^{-1}) along the harvest-riparian edge, and (c) 3.7 mg m^{-2} min^{-1} (1.1–12.1 mg m^{-2} min^{-1}) in the riparian buffer (Fig. S3). Statistically, there was no evidence for differences in sediment yields between any of the plot positions.

While the general pattern in sediment concentration among plot positions remained the same during the wet rainfall simulations as the dry rainfall simulations—general harvest area > harvest-riparian edge > riparian buffer (Fig. 6)—variation in sediment concentrations among plot positions was somewhat weaker than observed under dry

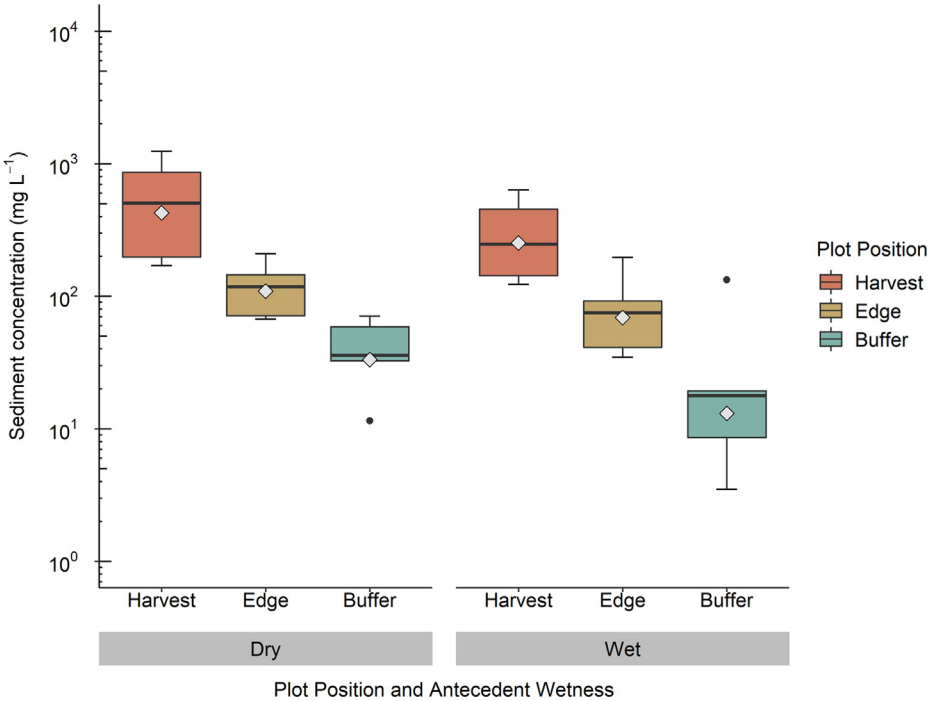

Fig. 6. Box-and-whisker plots of the average sediment concentration from plots in the general harvest area, at the riparian edge, and in the riparian buffer during the dry and wet rainfall simulations. Grey diamonds indicate the geometric means.

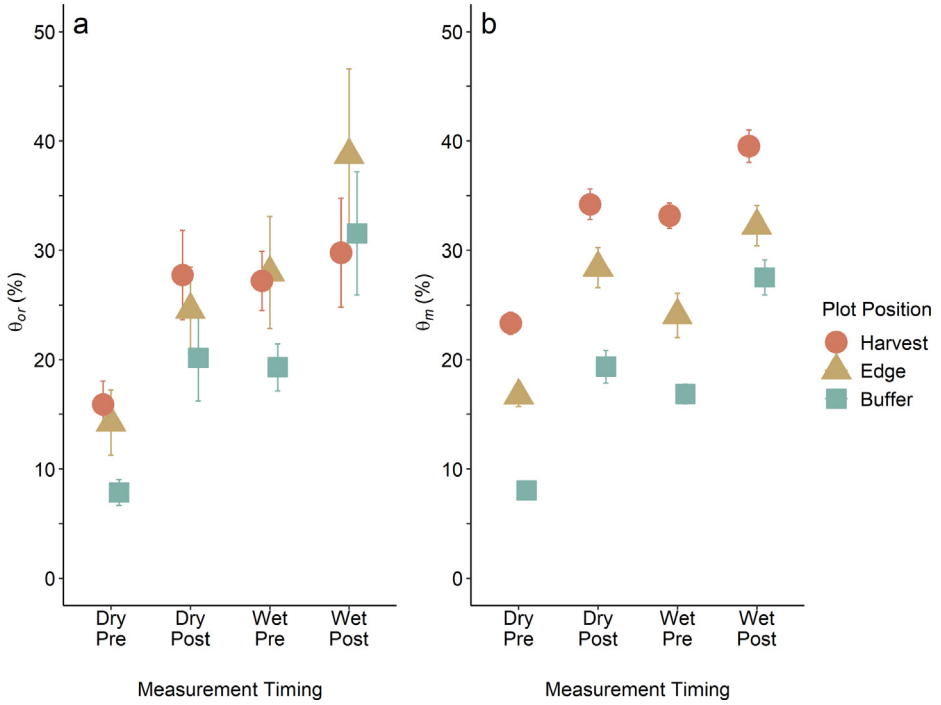

Fig. 7. Average volumetric water content (with standard errors) of the (a) organic (θ_{or}) and (b) upper 0–6 cm of the mineral soil (θ_m) from plots in the general harvest area, at the riparian edge, and in the riparian buffer under dry and wet antecedent moisture conditions.

rainfall simulations. The geometric mean and 95% confidence intervals (back-transformed) for the sediment concentration was (a) 285.7 mg l^{-1} (67.9–1201.5 mg l^{-1}) in the general harvest area, (b) 79.6 mg l^{-1} (36.5–173.5 mg l^{-1}) along the harvest-riparian edge, and (c) 22.3 mg l^{-1} (3.5–141.7 mg l^{-1}) in the riparian buffer. However, while sediment concentrations differed most strongly between the general harvest area and the riparian buffer ($t = 3.51$, $p = .01$), other pairwise comparisons were not significant ($p > .20$) as riparian-edge sediment concentrations during wet rainfall simulations were intermediate between those of the other two plot positions. The geometric mean and 95% confidence intervals (back-transformed) for the sediment yields during the wet simulations was (a) 3.0 mg m^{-2} min^{-1} (0.1–134.5 mg m^{-2} min^{-1}) in the general harvest area, (b) 2.3 mg m^{-2} min^{-1} (0.9–6.3 mg m^{-2} min^{-1}) along the harvest-riparian edge, and (c) 1.3 mg m^{-2} min^{-1} (0.2–9.3 mg m^{-2} min^{-1}) in the riparian buffer (Fig. S3). Statistically, there was no evidence for differences in sediment yields between any of the plot positions.

3.3. Soil water content

Prior to the dry condition rainfall simulations, mean volumetric water content of both the O-horizon (θ_{or}) and the upper 0–6 cm of the mineral soil (θ_m) generally followed the pattern of general harvest area > harvest-riparian edge > riparian buffer (Fig. 7a). However, variation in soil moisture among plot positions was weaker for θ_{or} than was evident for θ_m. While differences in θ_{or} were observed between the harvest area and the riparian buffer ($t = 2.55$, $p = .04$,), there was no evidence of differences in θ_{or} among the other plot positions ($p > .13$). However, we observed much stronger differences in θ_m between the harvest and the riparian buffer ($t = 15.42$, $p < .001$), and between the harvest-riparian edge and both the harvest area ($t = 5.16$, $p < .001$) and the riparian buffer ($t = 10.26$, $p < .001$).

The soil water content of the O-horizon (θ_{or}) increased from the dry condition simulation to the wet condition simulation by ~11.3% in the harvest area, ~14.5% at the harvest-riparian edge, and ~10.8% in the riparian buffer. Similarly, the soil water content of the upper 6 cm of mineral soil (θ_m) increased ~8.7% in the harvest area, ~5.1% at the harvest-riparian edge, and ~10.6% in the riparian buffer. Thus, prior to the wet condition rainfall simulations, both the θ_{or} and the θ_m followed the pattern of general harvest area > harvest-riparian edge > riparian buffer (Fig. 7b). However, while no statistically meaningful variation in θ_{or} was evident among plot positions ($p > .19$), much stronger effects of plot position were observed in deeper layers for θ_m ($p < .001$ for all pairwise comparisons).

4. Discussion

4.1. Runoff rates

Our study, in a high elevation Rocky Mountain catchment, demonstrated that surface and shallow subsurface runoff rates during high intensity rainfall events were greater in a riparian buffer relative to a recently harvested cutblock, especially when soil conditions were dry. This finding was counter to our expectation, as mechanical soil disturbance during forest harvesting activities has previously been associated with decreased porosity, infiltration capacity, and hydraulic conductivity, leading to intensified surface runoff (Birkinshaw et al., 2011; Huang et al., 1996; Malmer and Grip, 1990). However, after forest harvesting in Chile, Mohr et al. (2013) also observed higher infiltration and lower runoff rates in the general harvest area, which they partially attributed to the breakup of naturally occurring water-repellency at the soil surface and prolonged ponding of water due to increased soil surface roughness. In our study, we observed many depressions in microtopography in the general harvest area plots from mechanistic disturbance, which were not prevalent in the riparian buffer plots. Previous studies have illustrated that the presence of increased microtopographic variation can increase the proportion of precipitation infiltrating by 20–200 % (Dunne et al., 1991; Thompson et al., 2010). Indeed, in our study microtopography appeared to lead to greater ponding of water and infiltration in the plots in the harvest area compared to the riparian buffer. However, the effect of harvesting activity on surface microtopography was heterogeneous, especially at the harvest-riparian edge, which contributed to high variability in runoff response observed between plots.

Additionally, we postulate that the greater runoff volumes (Fig. 4) and shorter times to runoff initiation (Fig. S2) during the dry condition simulations and within the riparian buffer were strongly governed by the presence/absence of water repellency. We observed hydrophobic conditions most frequently during the dry condition rainfall simulations in the riparian buffer and, to a lesser extent, at the harvest-riparian edge. Specifically, we observed water visibly flowing along the organic horizon surface (above the mineral soil) shortly after the start of each rainfall simulation—we did not observe this phenomenon in the general harvest area. This is consistent with the presence of resins, waxes, or aromatic oils associated with pine-dominated forests and/or organic matter, which are most prevalent during hot, dry conditions and are known to increase runoff generation at the surface (Brown et al., 1999; Doerr et al., 2000; Kim et al., 2005; Miyata et al., 2007). These water repellent properties of the topsoil may have been broken up during forest harvesting or may have been reduced in the moister soils in harvested plots (Doerr et al., 2000), thereby increasing infiltration rates and reducing surface or shallow subsurface runoff in the harvested plots (Mohr et al., 2013).

The differences in runoff rates between the harvest area and the riparian buffer may also be partially attributable to differences in soil water content. Prior to the dry condition rainfall simulations, the volumetric water content in the upper horizons of the mineral soil was ~2.9-times greater in the harvest area compared to the riparian buffer. This finding is consistent with other studies, which have documented increased soil water content after forest harvesting because of strongly reduced rainfall interception and transpiration losses (Ares et al., 2005; Bethlahmy, 1962; Rab, 1996), including related research in our study catchments (Greenacre, 2019). Due to wetter soil conditions in the harvest area, initiation of preferential flow through larger macropores likely occurred more rapidly, enhancing vertical drainage and infiltration (Beven and Germann, 1982). Indeed, the greater infiltration we observed in the harvested area occurred despite much greater sediment entrainment in harvested plots, supporting the notion that preferential macropore flow (less susceptible to pore plugging) was the likely pathway responsible for enhanced drainage in harvested plots. In our study, shallow runoff rates decreased in all plots in the wet condition rainfall simulations relative to the dry condition simulations. This observation reinforces the idea of increased connection of pore networks as soil water content increases, resulting in greater and more rapid vertical flow (McDonnell, 1990; Sidle et al., 2000; Tsuboyama et al., 1994).

While we established transects and plots across a gradient of harvested to riparian settings, which had mostly similar environmental settings, unfortunately, there was a gradient of increasing slopes from harvested to riparian plots. This occurred because the harvested areas were constrained to gentler slopes less than 45%, which is typical for operations in high elevation, mountainous catchments. Despite this difference in plots, there was no clear reason to suspect slope had a major influence on infiltration or runoff from our small (1 m^2) plots. Rather, the well-established effects of water repellency and soil moisture on small plot infiltration-runoff were likely the more dominant factors (Mohr et al., 2013). Indeed, others have also observed the importance of microtopography, surface litter, and soil conditions (e.g., moisture content, bulk density) as dominant factors controlling infiltration and runoff at the small plot scale (Hartanto et al., 2003; Liu et al., 2019; Zhou et al., 2018). Moreover, Wu et al. (2017) recently noted that the role of slope on infiltration remains uncertain and a controversial issue even at the hillslope scale, with contrasting observations of increased runoff with increasing slope (Essig et al., 2009; Fox et al., 1997), decreased runoff with increasing slope (Abrahams et al., 1988; Assouline and Ben-Hur, 2006), or no relationship between runoff and slope (Cerdà and Garcia-Fayos, 1997; Grosh and Jarrett, 1994).

4.2. Sediment transfer

In our study, the geometric mean of the sediment concentrations in runoff from plots in the general harvest area was ~15.8-times greater than in the riparian buffer and ~4.2-times greater than at the harvest-riparian edge. Thus, it was apparent that forest harvesting activity increased sediment availability on hillslopes within the general harvest area, as observed previously in other experiments (Croke et al., 1999b). While the percent exposed bare soil in our harvested plots was only moderately greater than in the harvest-riparian edge or riparian area plots, drag scarification decreased soil aggregation and increased soil surface roughness in the harvested plots. Such effects on soil properties, would have increased hillslope sediment availability (Jordan et al., 2010). Within the limitations of the small (1 m^2) erosion plots in this study, the low runoff rates and high surface roughness in our general harvest area plots illustrated that the combination of greater particle detachment and initial sheet flow likely governed the greater sediment production from harvested plots. However, we also did not observe evidence of larger scale erosional features associated with broader concentrated surface flow or uniform sheet flow in the harvested areas known to entrain and redistribute sediment down hillslopes (Croke et al., 2005; Hairsine et al., 2002; Lakel et al., 2010; Neary et al., 2009; Rivenbark and Jackson, 2004). The low sediment concentrations in the riparian buffer plots may be attributable to surface runoff occurring at the duff/litter layer (above mineral soil). The cover and surface roughness provided by the litter layer is often a dominant control on surface erosion in forested environments (Ghahramani and Ishikawa, 2013; Powers, 2002; Stuart and Edwards, 2006). As such, while there was a clear gradient in mean plot slope from riparian buffers > riparian-harvest edges > harvested areas, our results for sediment production showed the opposite pattern, which supports the notion that the first order controls governing sediment production in this study were surface cover, litter, and soil exposure.

Sediment concentrations decreased during the wet condition rainfall simulation in all of the plots in the general harvest area and along the harvest-riparian edge. We attribute this surprising result to the removal of the loose sediment supply during the initial, dry condition rainfall simulation (Croke et al., 1999b). High surface roughness in the harvest area plots may also have contributed to moderately low sediment transport during the wet condition simulations (Bryan, 2000). Despite these observations, we caution that scale effects from plots are typically more variable for erosion than runoff, with sediment concentrations generally increasing with plot length along the hillslope (Bagarello and Ferro, 2017). Given that most observations and model simulations indicate higher erosion rates during high intensity precipitation events (Praskievicz, 2016; Routschek et al., 2014), it is critical to continue to improve our understanding of the drivers of erosional processes and sediment delivery to streams under these rare conditions at a range of spatial scales.

Our study also provides mechanistic insights into functional roles of riparian buffers in the broader suite of best management practices (BMPs) often employed in forest harvest operations. Many agencies describe one of the functions of riparian buffers as “filter-strips” that serve to limit sediment transfer from harvested areas to receiving streams. However, considerable historic and contemporary research indicates forest soils typically have high infiltration capacities, which rarely enable substantial surface runoff and sediment transfer into riparian reserves after harvesting (Litschert and MacDonald, 2009). Indeed, even under the extreme precipitation intensities employed in this study (> 100 yr. return period I_{60}), high surface roughness in the general harvest area promoted higher infiltration, and both lower surface runoff and runoff ratios in the general harvest area, which would make sediment penetration into or through riparian buffers highly unlikely in this setting.

5. Conclusions

Understanding the potential for surface or shallow subsurface runoff and erosion during infrequent, high intensity precipitation is critical given the projections for greater occurrence of these events in the future due to climate change. Observation of these rare events is difficult; however, the data from our rainfall simulations indicate such events may produce moderate surface/shallow subsurface runoff rates (~17.6–105.4 mm h^{-1}) in high elevation Rocky Mountain catchments. Forest harvesting activity appeared to result in higher infiltration rates and vertical, preferential flow compared to the riparian buffer. In contrast, the surface/shallow subsurface runoff rates were highest in the riparian buffer, which was likely due to differences in hydrophobicity, surface roughness, and soil water content between the sites. We also found differences in sediment concentrations—the highest sediment concentrations were from the general harvest area plots. Surprisingly, sediment concentrations decreased during the wet condition rainfall simulation relative to the dry condition rainfall simulations, especially in the general harvest area. This was likely due to exhaustion of a sediment supply, reduced connectivity due to surface roughness, and increased vertical, preferential flow with increasing soil wetness. Overall, while we observed moderately high variability in this plot scale study with only modest replication, the spatial patterns in runoff generation (both amount and timing of runoff initiation), sediment production, and their relationships with soil moisture were consistent and monotonic along the gradient from harvested areas through riparian buffers. This highlights the need for additional research to further explore if similar patterns appear evident in other hydro-climatic settings. Ultimately, a better understanding of mechanisms that regulate efficacy of best management practices such as riparian buffers, will contribute to continued improvements in practices for watershed protection.

CRediT authorship contribution statement

Kira C. Puntenney-Desmond: Conceptualization, Methodology, Formal analysis, Investigation, Writing - original draft, Writing - review & editing, Visualization. **Kevin D. Bladon:** Conceptualization, Methodology, Investigation, Resources, Writing - original draft, Writing - review & editing, Visualization, Supervision, Project administration, Funding acquisition. **Uldis Silins:** Conceptualization, Resources, Writing - review & editing, Supervision, Project administration, Funding acquisition.

Declaration of Competing Interest

The authors declare that they have no known competing financial interests or personal relationships that could have appeared to influence the work reported in this paper.

Acknowledgements

The research was funded by the Natural Sciences and Engineering Research Council (NSERC) of Canada, Alberta Agriculture and Forestry (Forest Management Branch), Alberta Innovates, Canfor, Forest Resource Improvement Association of Alberta, Oregon State University College of Forestry, Oregon Lottery Graduate Scholarship, and the Oregon State University General Research Fund. The authors are grateful to Chris Williams, Ryan Cole, Amanda Martens, Eric Lastiwka, Kalli Herlein, Chrystyn Skinner, Shauna Stack, Amelia Corrigan, Noah Kanzig, and Adrian Gallo for field and laboratory assistance.

Appendix A. Supplementary data

Supplementary data to this article can be found online at https://doi.org/10.1016/j.jhydrol.2019.124452.

References

Abrahams, A.D., Parsons, A.J., Luk, S.H., 1988. Hydrologic and sediment responses to simulated rainfall on desert hillslopes in southern Arizona. Catena 15 (2), 103–117. https://doi.org/10.1016/0341-8162(88)90022-7.

Amaranthus, M.P., Rice, R.M., Barr, N.R., Ziemer, R.R., 1985. Logging and forest roads related to increased debris slides in southwestern Oregon. J. For. 83 (4), 229–233. https://doi.org/10.1093/jof/83.4.229.

Ampoorter, E., de Schrijver, A., van Nevel, L., Hermy, M., Verheyen, K., 2012. Impact of mechanized harvesting on compaction of sandy and clayey forest soils: results of a meta-analysis. Ann. For. Sci. 69 (5), 533–542. https://doi.org/10.1007/s13595-012-0199-y.

Ares, A., Terry, T.A., Miller, R.E., Anderson, H.W., Flaming, B.L., 2005. Ground-based forest harvesting effects on soil physical properties and Douglas-fir growth. Soil Sci. Soc. Am. J. 69 (6), 1822–1832. https://doi.org/10.2136/sssaj2004.0331.

Assouline, S., Ben-Hur, A., 2006. Effects of rainfall intensity and slope gradient on the dynamics of interrill erosion during soil surface sealing. Catena 66 (3), 211–220. https://doi.org/10.1016/j.catena.2006.02.005.

Bagarello, V., Ferro, V., 2017. Scale effects on plot runoff and soil erosion in a Mediterranean environment. Vadose Zone J. 16 (12), 14. https://doi.org/10.2136/vzj2017.03.0059.

Benda, L., Hassan, M.A., Church, M., May, C.L., 2005. Geomorphology of steepland headwaters: The transition from hillslopes to channels. J. Am. Water Resour. Assoc. 41 (4), 835–851. https://doi.org/10.1111/j.1752-1688.2005.tb03773.x.

Bethlahmy, N., 1962. First year effects of timber removal on soil moisture. Hydrol. Sci. J. 7 (2), 34–38. https://doi.org/10.1080/02626666209493253.

Beven, K., Germann, P., 1982. Macropores and water flow in soils. Water Resour. Res. 18 (5), 1311–1325. https://doi.org/10.1029/WR018i005p01311.

Birkinshaw, S.J., Bathurst, J.C., Iroume, A., Palacios, H., 2011. The effect of forest cover on peak flow and sediment discharge-an integrated field and modelling study in central-southern Chile. Hydrol. Process. 25 (8), 1284–1297. https://doi.org/10.1002/hyp.7900.

Bladon, K.D., Bywater-Reyes, S., LeBoldus, J.M., Keriö, S., Segura, C., Ritóková, G., Shaw, D.C., 2019. Increased streamflow in catchments affected by a forest disease epidemic. Sci. Total Environ. 691, 112–123. https://doi.org/10.1016/j.scitotenv.2019.07.127.

Bonham, C.D., 2013. In: Measurements for Terrestrial Vegetation. Wiley, New York, NY, pp. 246. https://doi.org/10.1002/9781118534540.

Bosch, J.M., Hewlett, J.D., 1982. A review of catchment experiments to determine the effect of vegetation changes on water yield and evapotranspiration. J. Hydrol. 55 (1–4), 3–23. https://doi.org/10.1016/0022-1694(82)90117-2.

Brardinoni, F., Slaymaker, O., Hassan, M.A., 2003. Landslide inventory in a rugged forested watershed: a comparison between air-photo and field survey data. Geomorphology 54 (3–4), 179–196. https://doi.org/10.1016/s0169-555x(02)00355-0.

Brown, A.E., Zhang, L., McMahon, T.A., Western, A.W., Vertessy, R.A., 2005. A review of paired catchment studies for determining changes in water yield resulting from alterations in vegetation. J. Hydrol. 310 (1–4), 28–61. https://doi.org/10.1016/j.jhydrol.2004.12.010.

Brown, G.W., Krygier, J.T., 1971. Clear-cut logging and sediment production in Oregon Coast Range. Water Resour. Res. 7 (5), 1189–1198. https://doi.org/10.1029/WR007i005p01189.

Brown, V.A., McDonnell, J.J., Burns, D.A., Kendall, C., 1999. The role of event water, rapid shallow flowpaths and catchment size in summer stormflow. J. Hydrol. 217 (3–4), 171–190. https://doi.org/10.1016/S0022-1694(98)00247-9.

Bryan, R.B., 2000. Soil erodibility and processes of water erosion on hillslope. Geomorphology 32 (3–4), 385–415. https://doi.org/10.1016/s0169-555x(99)00105-1.

Bywater-Reyes, S., Segura, C., Bladon, K.D., 2017. Geology and geomorphology control suspended sediment yield and modulate increases following timber harvest in Oregon headwater streams. J. Hydrol. 548, 754–769. https://doi.org/10.1016/j.jhydrol.2017.03.048.

Cerdà, A., Garcia-Fayos, P., 1997. The influence of slope angle on sediment, water and seed losses on badland landscapes. Geomorphology 18 (2), 77–90. https://doi.org/10.1016/s0169-555x(96)00019-0.

Covert, A., Jordan, P., 2009. A portable rainfall simulator: techniques for understanding the effects of rainfall on soil erodibility. Streamline 13 (1), 5–9.

Cristan, R., Aust, W.M., Bolding, M.C., Barrett, S.M., Munsell, J.F., Schilling, E., 2016. Effectiveness of forestry best management practices in the United States: literature review. For. Ecol. Manage. 360, 133–151. https://doi.org/10.1016/j.foreco.2015.10.025.

Croke, J., Hairsine, P., Fogarty, P., 1999a. Runoff generation and re-distribution in logged eucalyptus forests, south-eastern Australia. J. Hydrol. 216 (1–2), 56–77. https://doi.org/10.1016/s0022-1694(98)00288-1.

Croke, J., Hairsine, P., Fogarty, P., 1999b. Sediment transport, redistribution and storage on logged forest hillslopes in south-eastern Australia. Hydrol. Process. 13 (17), 2705–2720. https://doi.org/10.1002/(sici)1099-1085(19991215)13:17<2705::aid-hyp843>3.0.co;2-y.

Croke, J., Mockler, S., Fogarty, P., Takken, I., 2005. Sediment concentration changes in runoff pathways from a forest road network and the resultant spatial pattern of catchment connectivity. Geomorphology 68 (3–4), 257–268. https://doi.org/10.1016/j.geomorph.2004.11.020.

Doerr, S.H., Shakesby, R.A., Walsh, R.P.D., 2000. Soil water repellency: its causes, characteristics and hydro-geomorphological significance. Earth-Sci. Rev. 51 (1–4), 33–65. https://doi.org/10.1016/s0012-8252(00)00011-8.

Dunne, T., Zhang, W.H., Aubry, B.F., 1991. Effects of rainfall, vegetation, and

microtopography on infiltration and runoff. Water Resour. Res. 27 (9), 2271–2285. https://doi.org/10.1029/91wr01585.
Easterling, D.R., Meehl, G.A., Parmesan, C., Changnon, S.A., Karl, T.R., Mearns, L.O., 2000. Climate extremes: observations, modeling, and impacts. Science 289 (5487), 2068–2074. https://doi.org/10.1126/science.289.5487.2068.
Ebel, B.A., Mirus, B.B., 2014. Disturbance hydrology: challenges and opportunities. Hydrol. Process. 28 (19), 5140–5148. https://doi.org/10.1002/hyp.10256.
Emelko, M.B., Silins, U., Bladon, K.D., Stone, M., 2011. Implications of land disturbance on drinking water treatability in a changing climate: demonstrating the need for "source water supply and protection" strategies. Water Res. 45 (2), 461–472. https://doi.org/10.1016/j.watres.2010.08.051.
Emelko, M.B., Stone, M., Silins, U., Allin, D., Collins, A.L., Williams, C.H.S., Martens, A.M., Bladon, K.D., 2016. Sediment-phosphorus dynamics can shift aquatic ecology and cause downstream legacy effects after wildfire in large river systems. Glob. Chang. Biol. 22 (3), 1168–1184. https://doi.org/10.1111/gcb.13073.
Essig, E.T., Corradini, C., Morbidelli, R., Govindaraju, R.S., 2009. Infiltration and deep flow over sloping surfaces: comparison of numerical and experimental results. J. Hydrol. 374 (1–2), 30–42. https://doi.org/10.1016/j.jhydrol.2009.05.017.
Fox, D.M., Bryan, R.B., Price, A.G., 1997. The influence of slope angle on final infiltration rate for interrill conditions. Geoderma 80 (1–2), 181–194. https://doi.org/10.1016/s0016-7061(97)00075-x.
Fredriksen, R.L., 1970. Erosion and sedimentation following road construction and timber harvest on unstable soils in three small western Oregon watersheds, U.S. Department of Agriculture, Forest Service, Pacific Northwest Forest and Range Experiment Station, Portland, OR.
Gee, G.W., Or, D., 2002. 2.4 Particle-size analysis. In: Dane, J.H., Topp, C. (Eds.), Methods of Soil Analysis. Part 4. Physical Methods. Soil Science Society of America Book Series, Madison, WI, pp. 255–278.
Ghahramani, A., Ishikawa, Y., 2013. Water flux and sediment transport within a forested landscape: the role of connectivity, subsurface flow, and slope length scale on transport mechanism. Hydrol. Process. 27 (26), 4091–4102. https://doi.org/10.1002/hyp.9791.
Goode, J.R., Luce, C.H., Buffington, J.M., 2012. Enhanced sediment delivery in a changing climate in semi-arid mountain basins: implications for water resource management and aquatic habitat in the northern Rocky Mountains. Geomorphology 139, 1–15. https://doi.org/10.1016/j.geomorph.2011.06.021.
Gray, D.H., Megahan, W.F., 1981. Forest vegetation removal and slope stability in the Idaho Batholith, U.S. Dept. of Agriculture, Forest Service, Intermountain Forest and Range Experiment Station, Ogden, UT.
Greenacre, D.M.E., 2019. Effects of Alternative Forest Harvesting Strategies on snowpack Dynamics and Seasonal Soil Moisture Storage in Alberta's Mountain Headwaters. University of Alberta, Edmonton, AB.
Grosh, J.L., Jarrett, A.R., 1994. Interrill erosion and runoff on very steep slopes. Trans. ASAE 37 (4), 1127–1133. https://doi.org/10.13031/2013.28186.
Hairsine, P.B., Croke, J.C., Mathews, H., Fogarty, P., Mockler, S.P., 2002. Modelling plumes of overland flow from logging tracks. Hydrol. Process. 16 (12), 2311–2327. https://doi.org/10.1002/hyp.1002.
Hallema, D.W., Sun, G., Bladon, K.D., Norman, S.P., Caldwell, P.V., Liu, Y., McNulty, S.G., 2017. Regional patterns of post-wildfire streamflow in the western United States: the importance of scale-specific connectivity. Hydrol. Process. 31 (14), 2582–2598. https://doi.org/10.1002/hyp.11208.
Harris, D.D., 1977. Hydrologic Changes after Logging in Two Small Oregon Coastal Watersheds. U.S Geological Survey, Washington, DC.
Hartanto, H., Prabhu, R., Widayat, A.S.E., Asdak, C., 2003. Factors affecting runoff and soil erosion: plot-level soil loss monitoring for assessing sustainability of forest management. For. Ecol. Manage. 180 (1–3), 361–374. https://doi.org/10.1016/s0378-1127(02)00656-4.
Hatten, J.A., Segura, C., Bladon, K.D., Hale, V.C., Ice, G.G., Stednick, J.D., 2018. Effects of contemporary forest harvesting on suspended sediment in the Oregon Coast Range: Alsea Watershed Study Revisited. For. Ecol. Manage. 408, 238–248. https://doi.org/10.1016/j.foreco.2017.10.049.
Huang, J., Lacey, S.T., Ryan, P.J., 1996. Impact of forest harvesting on the hydraulic properties of surface soil. Soil Sci. 161 (2), 79–86. https://doi.org/10.1097/00010694-199602000-00001.
Jones, J.A., Creed, I.F., Hatcher, K.L., Warren, R.J., Adams, M.B., Benson, M.H., Boose, E., Brown, W.A., Campbell, J.L., Covich, A., Clow, D.W., Dahm, C.N., Elder, K., Ford, C.R., Grimm, N.B., Henshaw, D.L., Larson, K.L., Miles, E.S., Miles, K.M., Sebestyen, S.D., Spargo, A.T., Stone, A.B., Vose, J.M., Williams, M.W., 2012. Ecosystem processes and human influences regulate streamflow response to climate change at long-term ecological research sites. Bioscience 62 (4), 390–404. https://doi.org/10.1525/bio.2012.62.4.10.
Jordan, P., Millard, T.H., Campbell, D., Schwab, J.W., Wilford, D.J., Nicol, D., Collins, D., 2010. Forest management effects on hillslope processes. In: Pike, R.G., Redding, T.E., Moore, R.D., Winkler, R.D., Bladon, K.D. (Eds.), Compendium of Forest Hydrology and Geomorphology in British Columbia. British Columbia Ministry of Forests and Range, Victoria, B.C., pp. 275–329.
Kim, H.J., Sidle, R.C., Moore, R.D., 2005. Shallow lateral flow from a forested hillslope: influence of antecedent wetness. Catena 60 (3), 293–306. https://doi.org/10.1016/j.catena.2004.12.005.
Lakel, W.A., Aust, W.M., Bolding, M.C., Dolloff, C.A., Keyser, P., Feldt, R., 2010. Sediment trapping by streamside management zones of various widths after forest harvest and site preparation. For. Sci. 56 (6), 541–551.
Litschert, S.E., MacDonald, L.H., 2009. Frequency and characteristics of sediment delivery pathways from forest harvest units to streams. For. Ecol. Manage. 259 (2), 143–150. https://doi.org/10.1016/j.foreco.2009.09.038.
Liu, J.K., Engel, B.A., Wang, Y., Zhang, Z.M., Zhang, M.X., 2019. Runoff response to soil moisture and micro-topographic structure on the plot scale. Sci. Rep. 9, 13. https://doi.org/10.1038/s41598-019-39409-6.
Luce, C.H., 2002. Hydrological processes and pathways affected by forest roads: what do we still need to learn? Hydrol. Process. 16 (14), 2901–2904. https://doi.org/10.1002/hyp.5061.
Luce, C.H., Black, T.A., 1999. Sediment production from forest roads in western Oregon. Water Resour. Res. 35 (8), 2561–2570. https://doi.org/10.1029/1999wr900135.
Macdonald, J.S., Beaudry, P.G., MacIsaac, E.A., Herunter, H.E., 2003. The effects of forest harvesting and best management practices on streamflow and suspended sediment concentrations during snowmelt in headwater streams in sub-boreal forests of British Columbia, Canada. Can. J. For. Res. 33 (8), 1397–1407. https://doi.org/10.1139/X03-110.
MacDonald, L.H., Sampson, R.W., Anderson, D.M., 2001. Runoff and road erosion at the plot and road segment scales, St John, US Virgin Islands. Earth Surf. Process. Landf. 26 (3), 251–272. https://doi.org/10.1002/1096-9837(200103)26:3<251::aid-esp173>3.3.co;2-o.
Mahat, V., Anderson, A., 2013. Impacts of climate and catastrophic forest changes on streamflow and water balance in a mountainous headwater stream in Southern Alberta. Hydrol. Earth Syst. Sci. 17 (12), 4941–4956. https://doi.org/10.5194/hess-17-4941-2013.
Malmer, A., Grip, H., 1990. Soil disturbance and loss of infiltrability caused by mechanized and manual extraction of tropical rain-forest in Sabah, Malaysia. For. Ecol. Manage. 38 (1–2), 1–12. https://doi.org/10.1016/0378-1127(90)90081-l.
McDonnell, J.J., 1990. A rationale for old water discharge through macropores in a steep, humid catchment. Water Resour. Res. 26 (11), 2821–2832. https://doi.org/10.1029/WR026i011p02821.
Miller, R.E., Scott, W., Hazard, J.H., 1996. Soil compaction and conifer growth after tractor yarding at three coastal Washingon locations. Can J. For. Res. 26 (2), 225–236. https://doi.org/10.1139/x26-026.
Mirus, B.B., Ebel, B.A., Mohr, C.H., Zegre, N., 2017. Disturbance hydrology: preparing for an increasingly disturbed future. Water Resour. Res. 53 (12), 10007–10016. https://doi.org/10.1002/2017WR021084.
Miyata, S., Kosugi, K., Gomi, T., Onda, Y., Mizuyama, T., 2007. Surface runoff as affected by soil water repellency in a Japanese cypress forest. Hydrol. Process. 21 (17), 2365–2376. https://doi.org/10.1002/hyp.6749.
Mohr, C.H., Coppus, R., Iroume, A., Huber, A., Bronstert, A., 2013. Runoff generation and soil erosion processes after clear cutting. J. Geophys. Res.-Earth Surf. 118 (2), 814–831. https://doi.org/10.1002/jgrf.20047.
Moore, R.D., Wondzell, S.M., 2005. Physical hydrology and the effects of forest harvesting in the Pacific Northwest: a review. J. Am. Water Resour. Assoc. 41 (4), 763–784. https://doi.org/10.1111/j.1752-1688.2005.tb03770.x.
Motha, J.A., Wallbrink, P.J., Hairsine, P.B., Grayson, R.B., 2003. Determining the sources of suspended sediment in a forested catchment in southeastern Australia. Water Resour. Res. 39 (3), 14. https://doi.org/10.1029/2001wr000794.
Nearing, M.A., Pruski, F.F., O'Neal, M.R., 2004. Expected climate change impacts on soil erosion rates: a review. J. Soil Water Conserv. 59 (1), 43–50.
Neary, D.G., Ice, G.G., Jackson, C.R., 2009. Linkages between forest soils and water quality and quantity. For. Ecol. Manage. 258 (10), 2269–2281. https://doi.org/10.1016/j.foreco.2009.05.027.
Oyarzun, C.E., Pena, L., 1995. Soil-erosion and overland-flow in forested areas with pine plantations at coastal mountain-range, central Chile. Hydrol. Process. 9 (1), 111–118. https://doi.org/10.1002/hyp.3360090110.
Powers, R.F., 2002. Effects of soil disturbance on the fundamental, sustainable productivity of managed forests. In: Verner, J. (Ed.), Proceedings of a Symposium on the Kings River Sustainable Forest Ecosystem Project: Progress and Current Status. Pacific Southwest Research Station, Forest Service, U.S. Department of Agriculture, Albany, CA, pp. 63-82.
Praskievicz, S., 2016. Modeling hillslope sediment yield using rainfall simulator field experiments and partial least squares regression: Cahaba River watershed, Alabama (USA). Environ. Earth Sci. 75 (19), 15. https://doi.org/10.1007/s12665-016-6149-5.
R Core Team, 2017. R: A Language and Environment for Statistical Computing. R Foundation for Statistical Computing, Vienna, Austria.
Rab, M.A., 1996. Soil physical and hydrological properties following logging and slash burning in the Eucalyptus regnans forest of southeastern Australia. For. Ecol. Manage. 84 (1–3), 159–176. https://doi.org/10.1016/0378-1127(96)03740-1.
Ramos, M.C., Martinez-Casasnovas, J.A., 2015. Climate change influence on runoff and soil losses in a rainfed basin with Mediterranean climate. Nat. Hazards 78 (2), 1065–1089. https://doi.org/10.1007/s11069-015-1759-x.
Rivenbark, B.L., Jackson, C.R., 2004. Concentrated flow breakthroughs moving through silvicultural streamside management zones: Southeastern Piedmont, USA. J. Am. Water Resour. Assoc. 40 (4), 1043–1052. https://doi.org/10.1111/j.1752-1688.2004.tb01065.x.
Routschek, A., Schmidt, J., Kreienkamp, F., 2014. Impact of climate change on soil erosion - a high-resolution projection on catchment scale until 2100 in Saxony/Germany. Catena 121, 99–109. https://doi.org/10.1016/j.catena.2014.04.019.
Sheridan, G.J., Noske, P.J., Whipp, R.K., Wijesinghe, N., 2006. The effect of truck traffic and road water content on sediment delivery from unpaved forest roads. Hydrol. Process. 20 (8), 1683–1699. https://doi.org/10.1002/hyp.5966.
Sidle, R.C., Hirano, T., Gomi, T., Terajima, T., 2007. Hortonian overland flow from Japanese forest ptantations - an aberration, the real thing, or something in between? Hydrol. Process. 21 (23), 3237–3247. https://doi.org/10.1002/hyp.6876.
Sidle, R.C., Tsuboyama, Y., Noguchi, S., Hosoda, I., Fujieda, M., Shimizu, T., 2000. Stormflow generation in steep forested headwaters: a linked hydrogeomorphic paradigm. Hydrol. Process. 14 (3), 369–385. https://doi.org/10.1002/(SICI)1099-1085(20000228)14:3<369::AID-HYP943>3.0.CO;2-P.
Sidle, R.C., Ziegler, A.D., Negishi, J.N., Nik, A.R., Siew, R., Turkelboom, F., 2006. Erosion

processes in steep terrain - truths, myths, and uncertainties related to forest management in Southeast Asia. For. Ecol. Manage. 224 (1–2), 199–225. https://doi.org/10.1016/j.foreco.2005.12.019.

Silins, U., Anderson, A., Bladon, K.D., Emelko, M.B., Stone, M., Spencer, S.A., Williams, C.H.S., Wagner, M.J., Martens, A.M., Hawthorn, K., 2016. Southern Rockies Watershed Project. For. Chron. 92 (1), 39–42. https://doi.org/10.5558/tfc2016-012.

Silins, U., Stone, M., Emelko, M.B., Bladon, K.D., 2009. Sediment production following severe wildfire and post-fire salvage logging in the Rocky Mountain headwaters of the Oldman River Basin, Alberta. Catena 79 (3), 189–197. https://doi.org/10.1016/j.catena.2009.04.001.

Sosa-Perez, G., MacDonald, L.H., 2017. Effects of closed roads, traffic, and road decommissioning on infiltration and sediment production: a comparative study using rainfall simulations. Catena 159, 93–105. https://doi.org/10.1016/j.catena.2017.08.004.

Stednick, J.D., 1996. Monitoring the effects of timber harvest on annual water yield. J. Hydrol. 176 (1–4), 79–95. https://doi.org/10.1016/0022-1694(95)02780-7.

Stuart, G.W., Edwards, P.J., 2006. Concepts about forests and water. N. J. Appl. For. 23 (1), 11–19. https://doi.org/10.1093/njaf/23.1.11.

Thompson, S.E., Katul, G.G., Porporato, A., 2010. Role of microtopography in rainfall-runoff partitioning: an analysis using idealized geometry. Water Resour. Res. 46, 11. https://doi.org/10.1029/2009wr008835.

Trenberth, K.E., Dai, A., Rasmussen, R.M., Parsons, D.B., 2003. The changing character of precipitation. Bull. Am. Meteorol. Soc. 84 (9), 1205–1217. https://doi.org/10.1175/bams-84-9-1205.

Tsuboyama, Y., Sidle, R.C., Noguchi, S., Hosoda, I., 1994. Flow and solute transport through the soil matrix and macropores of a hillslope segment. Water Resour. Res. 30 (4), 879–890. https://doi.org/10.1029/93wr03245.

Wagner, M.J., Bladon, K.D., Silins, U., Williams, C.H.S., Martens, A.M., Boon, S., MacDonald, R.J., Stone, M., Emelko, M.B., Anderson, A., 2014. Catchment-scale stream temperature response to land disturbance by wildfire governed by surface-subsurface energy exchange and atmospheric controls. J. Hydrol. 517, 328–338. https://doi.org/10.1016/j.jhydrol.2014.05.006.

Wallbrink, P.J., Croke, J., 2002. A combined rainfall simulator and tracer approach to assess the role of Best Management Practices in minimising sediment redistribution and loss in forests after harvesting. For. Ecol. Manage. 170 (1–3), 217–232. https://doi.org/10.1016/S0378-1127(01)00765-4.

Wemple, B.C., Swanson, F.J., Jones, J.A., 2001. Forest roads and geomorphic process interactions, Cascade Range, Oregon. Earth Surf. Process. Landf. 26 (2), 191–204. https://doi.org/10.1002/1096-9837(200102)26:2<191::aid-esp175>3.0.co;2-u.

Wu, S.B., Yu, M.H., Chen, L., 2017. Nonmonotonic and spatial-temporal dynamic slope effects on soil erosion during rainfall-runoff processes. Water Resour. Res. 53 (2), 1369–1389. https://doi.org/10.1002/2016wr019254.

Zhou, Q.W., Zhou, X., Luo, Y., Cai, M.Y., 2018. The effects of litter layer and topsoil on surface runoff during simulated rainfall in Guizhou Province, China: a plot scale case study. Water 10 (7), 11. https://doi.org/10.3390/w10070915.